JOURNAL OF CATALYSIS 49, 97–108 (1977)

Ruthenium Zeolite Catalysts

A Characterization by Gas Adsorption, Thermogravimetry and Catalytic Activity for the Hydrogenation of Benzene

BRENDAN COUGHLAN, S. NARAYANAN, WILLIAM A. MCCANN, AND WILLIAM M. CARROLL

Physical Chemistry Laboratories, University College, Galway, Ireland

Received February 8, 1977

Several ruthenium A, X, Y, L, and mordenite zeolites have been prepared and characterized. The ruthenium zeolites have been studied by thermogravimetry and adsorption techniques and their catalytic activity for the hydrogenation of benzene in the range 353–433 K has been investigated. All the zeolites retain their crystalline structure after several outgassings at 623 K and sorption of CO_2; they are also stable to reduction at 723 K in flowing hydrogen. Turnover numbers for benzene hydrogenation increase smoothly with increasing metal surface area in all the zeolites.

INTRODUCTION

Over the past decade there has been a very lively growth of interest in homoionic and heteroionic zeolite catalysts; zeolitic frameworks have been shown to be active and thermally stable matrices for carrying transition metal species whose catalytic activity has hitherto been studied in alloys or on supports and carriers such as silica, alumina, silica–alumina and silica–magnesia. Zeolites, because of their bifunctional catalytic behavior and higher activity and better tolerance to sulfur and nitrogen poisoning than the conventional amorphous supports, are widely used in various petroleum reforming processes and a number of comprehensive reviews (*1–6*) describing zeolite-based catalysis have been published.

In the present paper we report the preparation of several ruthenium loaded zeolite catalysts with widely different cation densities, cation-binding energies, pore structures and molecular sieve properties and we discuss their activity for the reduction of benzene; we also report on their thermal stability and on their sorption properties towards carbon dioxide. The carbon dioxide molecule has already been shown (*7–11*) to be a useful probe for determining the specificity of sorption and accessibility of cations in zeolites. Virtually nothing has been published on the catalytic activity of zeolitic ruthenium although ruthenium carried on other supports is known to catalyze a variety of reactions: e.g., metallic ruthenium possesses high and stable activity for steam reformation of methane (*12*); phosphine complexes of ruthenium bonded to a silica surface catalyze the hydrogenation of olefins and dienes (*13*) and ruthenium supported on Al_2O_3 catalyzes the methanation of CO (*14*). Sinfelt and Yates (*15*) and Lam and Sinfelt (*16*) have reported hydrogenolysis of ethane and dehydrogenation of cyclohexane on $Ru–SiO_2$ and dehydrogenation and hydrogenolysis of *n*-pentane over

ISSN 0021-9517

$Ru–Al_2O_3$ has also been reported. Amano and Parravano (*18*) have studied the kinetics of hydrogenation of benzene on ruthenium, rhodium, palladium and platinum catalysts supported on alumina and observed the activity sequence: Rh > Ru > Pt > Pd; Kubicka (*19*) has reported the sequences Ru > Pt > Tc ≈ Pd > Re and Ru > Tc > Re, respectively, for the hydrogenation and hydrogenolysis of benzene when the metals were supported on silica and γ-alumina. Klimisch and Taylor (*20*) in a series of papers have reported on the activity of Ru supported on alumina in the reduction of nitric oxide to nitrogen in feed streams resembling automotive exhaust: the Ru catalysts were very selective and the formation of ammonia, a major fault of other catalysts, was minimized. As outlined in these representative reactions the well-established catalytic activity of Ru on the one hand and the versatility and thermal stability of certain zeolite frameworks as catalyst supports, on the other, make this investigation of the properties of zeolite ruthenium catalysts timely. The activity of other metals also in benzene reduction are referred to below.

EXPERIMENTAL METHODS

Catalyst Preparation

The catalysts, a summary of the preparative conditions and their compositions are listed in Table 1. The composition of the parent zeolites was

X: $Na_{86}(AlO_2)_{86}(SiO_2)_{106}$ 264 H_2O;

Y: $Na_{56}(AlO_2)_{56}(SiO_2)_{136}$ 250 H_2O;

A: $Na_{12}(AlO_2)_{12}(SiO_2)_{12}$ 27 H_2O;

L: $K_8Na(AlO_2)_9(SiO_2)_{27}$ 21 H_2O;

mordenite = M: $Na_8(AlO_2)_8(SiO_2)_{40}$ 27 H_2O.

The preparation of samples A-1, A-2, X-1, X-2, Y-1, Y-2, L-1, and L-2, by ion exchange from aqueous solutions of $Ru(H_2O)^{3+}_6$ and their chemical analysis has been described previously (*21*). Samples L-4, Y-4 and M-4 were prepared by stirring the parent zeolites at room temperature in 0.05 mol dm^{-3} aqueous ruthenium trichloride solutions for 10 min followed by filtration and thorough washing with hot deionized water. The samples were then dried at 383 K and pelletized without binder using a pressure of about 4000 kg cm^{-2}. The pellets were crushed and sieved and only particles of 1200–1600 μm were used for catalysis experiments.

Adsorption Studies

Sorption of carbon dioxide on samples X-1, Y-1, A-1, and L-1 was studied in the temperature range 273–473 K using the volumetric method as described previously (*7*). Prior to sorption experiments the samples were outgassed under vacuum at 633 K for a period of 12 hr. X-Ray diffraction patterns taken both before and after several outgassings and sorption of carbon dioxide showed no detectable loss of crystallinity. Calorimetric studies (*22*) of the immersion of outgassed samples in liquid water also gave heats of reasonable magnitude which would not be the case if there had been any appreciable crystal collapse. The water content of each sample (Table 1) was determined from the mass loss at 873 K using a Perkin–Elmer TGS 1 thermobalance; DTG curves for each sample were obtained using the same instrument; a heating rate of 20 K min^{-1} was employed in all the thermogravimetric work and a nitrogen flow of 25 cm^3 min^{-1} was maintained over the samples. The ruthenium metal surface area of each sample was measured by hydrogen adsorption after the catalysis experiment. Before the hydrogen adsorption measurements the catalysts were reduced in flowing hydrogen for 2 hr at 723 K, evacuated at 633 K for 1 hr and then cooled to 293 K, at which temperature the isotherms were measured; the uptake at 20 Torr was taken as a monolayer of hydrogen. The metal surface

TABLE 1

Analysis and Preparative Conditions of Ruthenium Zeolites

Zeolite sample	Exchange time/min	pH	Na^+ ions/ unit cell exchanged	Ruthenium ions/unit cell	Av charge/ ruthenium ion	Wt% ruthenium	% Mass loss
A-1	18	6.5	5.19	1.50	3.5	9.04	17.3
A-2	75	6.5	5.49	1.60	3.5	9.10	16.9
X-1	1080	6.5	45.21	38.30	1.2	24.20	24.1
X-2	45	6.5	48.13	19.70	2.4	13.90	23.2
Y-1	1080	6.5	15.01	7.30	2.1	5.40	22.2
Y-4	10	4.1	11.50	5.54	2.1	4.37	24.8
L-1	18	6.5	2.99[a]	0.96	3.1	4.31	9.8
L-2	45	6.5	3.04[a]	1.06	2.9	4.30	9.9
L-4	10	2.8	0.43[a]	0.13	3.2	0.85	12.4
M-1	1200	1.0	3.37	1.12	3.0	3.68	14.9
M-4	10	2.6	1.26	0.71	1.8	2.36	12.7

[a] $Na^+ + K^+$ ions exchanged

area (A) was calculated using 9.03×10^{-20} m^2 as the area of a Ru atom and by assuming that one hydrogen atom is adsorbed by each ruthenium metal atom.

The monolayer uptake per gram of catalyst, the dispersion of ruthenium and the crystallite sizes L are listed in Table 3. The crystallite sizes were calculated assuming the metal particles to be cubes of side L and with all faces accessible to hydrogen; the area (A) per gram of exposed metal is given by $6L^2n$, where n is the number of crystallites per gram. If $\rho(=12.2 \times 10^6$ kg $m^{-3})$ is the density of metallic ruthenium then $n = 1/\rho L^3$ and

$$L \text{ (in m)} = 6/\rho A = (4.918 \times 10^{-7})/A.$$

Catalysis Studies

The hydrogenation of benzene was carried out in the vapor phase at various temperatures in the range 353–433 K in flowing hydrogen (120 cm^3 min^{-1}). The catalyst particles were packed in an all glass vertical flow type reactor. The temperature of the catalyst bed was monitored using an iron–constantan thermocouple in conjunction with a digital voltmeter. The pretreatment of all the catalysts was the same: the fresh catalyst particles were reduced in flowing hydrogen (120 cm^3 min^{-1}) for 6 hr at 723 K; at the beginning of each experiment the catalyst was again activated in hydrogen with the same flow conditions, for 1 hr at 673 K. Liquid benzene was introduced at the top of the reactor using a calibrated motorized syringe and the product was collected in a trap immersed in ice. At the beginning of each run 10 min were allowed to elapse before any product was collected and then collection was continued for 1 hr. Catalytic activity did not change over this period; in the case of samples L-4 and M-4 activity was monitored over a period of 180 min by collecting products every 30 min; activity was found to be steady up to 150 min after which it began to decrease slowly to 95% conversion in the case of L-4 and to 90% for M-4 after 180 min. For all experiments the liquid product which contained only cyclohexane and any unreacted benzene was analyzed by glc. Turnover numbers (N), defined as the number of benzene molecules converted to cyclohexane per atom of exposed ruthenium metal per second, were calculated for each experiment. All samples were found by X-ray diffraction to have retained their crystal-

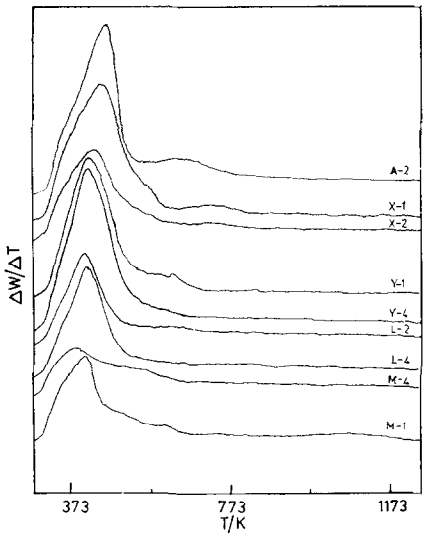

FIG. 1. DTG curves for ruthenium zeolites.

linity throughout the catalysis experiments and all the catalysis data were reproducible.

RESULTS AND DISCUSSION

Thermogravimetric Data

The compositions of the several ruthenium zeolites are given in Table 1. Ruthenium chemistry is complex and not nearly as well understood as that of most other transition metals and this introduces difficulties in the characterization of ruthenium zeolites. However of immediate interest are variations in the unit cell water contents, the average charge carried by the ruthenium ions (estimated from columns 4 and 5 of Table 1) and any inherent dependence of the properties of the resultant zeolite catalysts on the method of preparation. The percentage mass losses of the ruthenium zeolites, column 8, Table 1 are all less than those corresponding to the dehydration of the parent zeolites (parent A = 22.4%, X = 26.5%, Y = 26.5%, L = 13.4%, M = 13.7%) and in samples X-1, X-2, Y-1, Y-2, and M-4 the ruthenium ions have an average charge considerably less than 3. Absorption spectra of buffered exchanging $Ru(H_2O)^{3+}_6$ solutions showed a gradual decrease with time in the band at 225 nm with a corresponding increase in that at 260 nm; thus a change in the ligand field is reducing the energy of the $t^5_{2g} \leftarrow \pi$ transition and from the spectrochemical series this is consistent with a ligand change from H_2O to OH^-. Bearing in mind also that aqueous solutions of "ruthenium trichloride" contain Ru^{3+} and Ru^{4+} species (*23*) all the above evidence is in agreement with ion exchange of hydrolyzed ruthenium into the zeolites, the hydrolysis being extensive in the case of samples X-1, X-2, Y-1, Y-4, and M-4; the extent of hydrolysis in the A and L zeolite samples and in sample M-1 which was prepared at low pH is comparatively small. Samples L-4, Y-4, and M-4 were prepared from aqueous solutions of ruthenium trichloride which are known to be prone to hydrolysis (*24*) but it is not clear why the hydrolysis is greater in the case of the latter zeolite.

Minachev *et al.* (*25*) have shown that reduction of transition metal cations in zeolites is accompanied by migration of the metal to the external surface of the crystals and that the reduction depends on factors such as the chemical nature of the cation, the degree of ion exchange, cation location and the thermal stability of structural hydroxyls; therefore, it is to be expected that the dispersion of the reduced ruthenium in our zeolites would relate to the structure of the host lattice and the thermal stability of hydrolysis products. Representative DTG curves scanned in the temperature range 293–1273 K are shown for several ruthenium zeolites in Fig. 1 and the temperatures of the main peaks are listed in Table 2. In the analysis of the thermogravimetric data it should be borne in mind that the evidence outlined above supports the ideas that hydrolysis in the A, L, and M-4 samples is relatively small, that in the case of the X and Y samples hydroxyl groups are introduced by ion exchange of $Ru(OH)^{(3-x)+}_x$ species and

TABLE 2

DTG Features

Sample	T (K); peak:			% Mass loss			
	I	II	III	I	II	III	Total
A-2	400	573–773	—	14.5	2.4	—	16.9
X-1	429	653–773	853–933	22.3	1.0	0.8	24.1
X-2	413	653–773	—	22.2	0.9	—	23.1
Y-1	405	613	—	21.06	1.1	—	22.16
Y-4	405	—	—	24.8	—	—	24.8
L-2	397	613–693	—	8.88	1.0	—	9.88
L-4	397	—	—	12.4	—	—	12.4
M-1	401(493)	593	1013–1133	12.9	1.0	1.0	14.9
M-4	381(500)	—	—	12.7	—	—	12.7

that in the case of M-1, because of the low pH employed in preparation, some framework hydrolysis is likely (*26*). The DTG curve for sample A-1 (and A-2 which was similar) may be conveniently analyzed in the light of the work of Dyer and Wilson (*27*) who studied Na-A by TG, TMA, and DTA and that of Vucelic *et al.* (*28*) who studied Na-A by DSC. The main DTG peak centered at 400 K is a combination of two close peaks and may be attributed to the loss of structural water from the polylayer solvating the cations and to the loss of water bound by hydrogen bonds to the framework oxygens in the α cages; peak II represents the loss of more tightly bound water from the β cages over a long temperature interval and there is no further mass loss above 773 K. Sample M-1 has a dehydrogenation peak in the range 1013–1133 K and agrees well with that found at 1023 K by Weeks *et al.* (*29*) in their study of H-M; also characteristic (*22*, *29*) of mordenite samples in which framework hydrolysis has occurred, sample M-1 is more difficult to dehydrate compared with M-4 as is evident from the shifting of peaks I and II to higher temperatures. It is quite striking that sample M-4, in which the average charge per ruthenium ion is much less than 3, shows no evidence of dehydroxylation; therefore, it is to be expected that the hydrolysis products would have some bearing on the reduction of the ruthenium and the catalytic properties of this zeolite. Zeolites L-4 and Y-4 behave in a similar manner having peaks centered at 397 and 405 K, respectively, due to loss of molecular water and again do not suffer dehydroxylation at higher temperatures; the DTG curves for the parent L and Y zeolites also consist of a single peak at these temperatures (*10*, *30*). The remaining samples X-1, X-2, Y-1, and L-2 have in addition to peak I, which represents loosely held water, additional smaller peaks at higher temperatures; these peaks must represent the elimination of very tightly held water or dehydroxylation. The complexity of the dehydration process is shown by the fact that peak II corresponds to the elimination of approximately 12 H_2O molecules from X-1 and 9 H_2O from X-2 per unit cell even though the ruthenium in the former sample is considerably more hydrolyzed; sample X-1 also loses an additional 9 hydroxyl water molecules in the region 853–933 K (peak III) and this is borne out by the CO_2 sorption work below. The reason for the two sharp minima at 559 and 553 K in the curves for X-1 and X-2, respectively, is not clear; these were reproducible and may be due to the formation of an unstable Ru–nitrogen species.

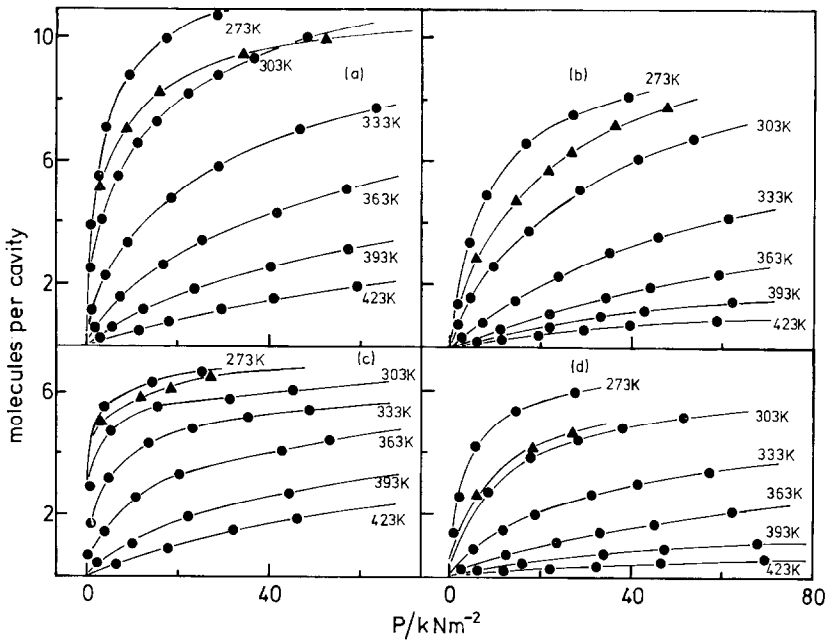

FIG. 2. Families of CO_2 isotherms for ruthenium zeolites X-1 (a); Y-1 (b); A-1 (c); and L-1 (d); (▲) isotherm for parent zeolite at 303 K.

CO_2 Adsorption Data

Families of CO_2 isotherms measured in the temperature range 273–423 K for samples X-1, Y-1, A-1, and L-1 are shown in Fig. 2; isotherms at 303 K for Na-X (*7*), Na-Y (*10*), Na-A (*9*), and K_9-L (*31*) are also included for comparison. All the zeolites sorb CO_2 copiously and the fact that the isotherms were reproducible is further evidence that ruthenium zeolites are stable to outgassing. Figure 3 is a comparison of sorption affinities, $\Delta\mu$ at 303.15 K defined by the relationship,

$$\Delta\mu = RT \ln p/p_0,$$

where p is the equilibrium pressure and p_0 is taken as 1 atm. At the lower coverages the affinity sequence is A-1 > X-1 > Y-1 ≈ L-1 but at the higher coverages X-1 is the best sorbent for CO_2. The affinity sequence at the lower coverages is the same order as the Al_2O_3:SiO_2 ratio or cation density and is also the same as that observed previously for other trivalent forms of these zeolites (*8*). CO_2 is a quadrupolar molecule and its sorption characteristics will reflect to a large extent the degree of interaction of its quadrupole with local electric field gradients generated by exposed cations. In Fig. 4 the CO_2 uptakes in samples X-1 and Y-1 at 303 K and 30 cm Hg are compared with those for the parent and variously exchanged Cr^{3+}, Y^{3+}, and Co^{3+} samples; the amounts sorbed are seen to decrease smoothly with increasing percentage of M^{3+} exchange in a manner which seems to be independent of the nature of the M^{3+} cation for both host lattices. The percentage exchange is defined here as the percentage of Na^+ ions in the parent zeolite replaced by the exchanging cation and according to this definition samples X-1 and Y-1 are 52.6 and 26.8% exchanged, respectively. The uptake on sample Y-1 under these conditions, 48 CO_2 molecules/unit cell, is seen to agree well with the curve for zeolite Y but that for sample X-1, 77 molecules/unit cell, falls well off

the corresponding curve for zeolite X. In fact the amount sorbed by sample X-1 is identical to that for Na-X and suggests strongly that the sorbate molecules in X-1 experience an environment more typical of that produced by monovalent cations than by multivalent ruthenium cations; such an effect would be in keeping with Table 1 where, due to hydrolysis, the average charge per ruthenium cation is estimated to be only slightly greater than unity. In a derivation of cation distributions for outgassed X and Y zeolites (*8*), decreasing CO_2 sorption with increasing exchange by trivalent cations has been attributed to migration of these cations to sites which are inaccessible to CO_2 (sites I, I′, and II′) with a consequent depopulation of accessible supercage sites. In the CO_2–Na-Y system the sorbate was considered to interact with 30 Na^+ ions distributed in supercage sites. The CO_2 molecule is too large to pass through the six-membered rings and gain entry to the sodalite cages; the reduced uptake in sample Y-1 compared with Na-Y may be attributed to a reduced

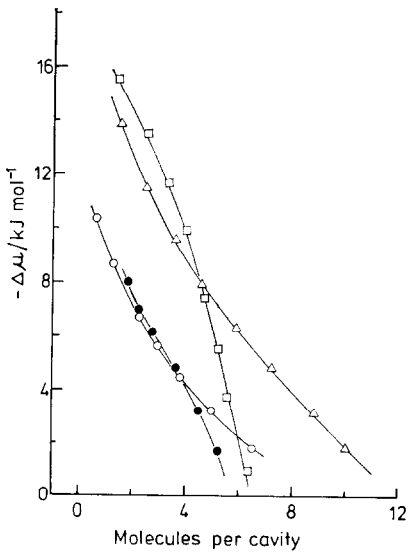

FIG. 3. Comparison of sorption affinities towards CO_2 in ruthenium zeolites X-1 (△); Y-1 (○); A-1 (□); and L-1 (●).

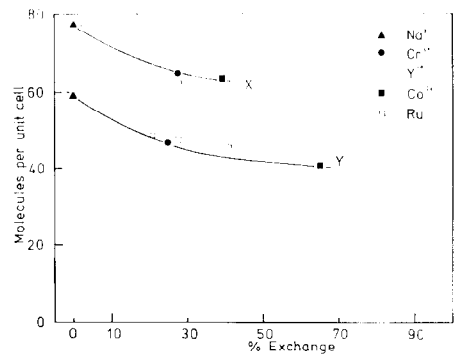

FIG. 4. Comparison of CO_2 uptakes in ruthenium X and Y zeolites at 303.15 K and 30 cm Hg (40 kN m^{-2}) with uptakes in the parent and trivalent exchanged zeolites.

number of cations interacting with the sorbate due to either a migration of ruthenium cations to inaccessible sites or to the presence of hydroxylated ruthenium in the supercages.

Catalysis Data

Table 3 summarizes the physical characteristics of the catalysts obtained from hydrogen chemisorption studies; examination of the table reveals that with the exception of the L-2 and A-2 samples the crystallite size increases and the surface area decreases smoothly with increasing ruthenium content. Crystal growth seems to occur much more readily in L-2 and A-2 than in the other samples; e.g., there is a very large difference in metal dispersion between samples L-2 and Y-4 which contain similar amounts of ruthenium. It is interesting to note that samples Y-1 and Y-4, which were prepared by different methods and which contain hydrolyzed ruthenium have similar metal crystallite sizes and also similar catalytic activity. As mentioned above the reduction of transition metal cations is likely to be accompanied by migration of the metal to the exterior of the zeolite crystals (*25*). Given migration, crystallite size or reduction cannot be a factor solely of the metal content. It is

TABLE 3

Hydrogen Adsorption Data

Catalyst	% by wt Ru	H_2 adsorption (μmoles g^{-1} of catalyst)	A (m^2 g^{-1} of Ru)	Dispersion (H/M)	Crystallite size L(nm)
A-2	9.10	25	30	0.055	16.3
X-1	24.2	280	126	0.234	3.8
X-2	13.9	170	133	0.247	3.6
Y-1	5.4	139	280	0.520	1.7
Y-4	4.4	119	295	0.550	1.6
L-2	4.3	35	88	0.165	5.5
L-4	0.85	43	537	1.00	0.9
M-4	2.36	68	313	0.584	1.5

likely to depend on factors such as the chemical nature of the cations, the Si/Al ratio or framework charge, the possibility of migration of the cations to hidden sites such as the hexagonal prisms in zeolites X and Y—a process which would be in competition with the reduction process, the location of cations in the lattice prior to reduction which would in turn depend on the level of exchange, the cation binding energy and cation-framework coordination, the degree of hydrolysis and the openness of the zeolite pore structure. The effect of the latter factor may be gauged from Table 4; in the less open A, M and L zeolites the chances of agglomeration of the metal atoms are considerably increased due to the greater relative proximity of the atoms. Minachev *et al.* (*25*) have reported the ability of reduced metals to migrate to the exterior surface of exchanged faujasites to decrease in the series: Ag > Zn > Pd > Cu > Ni > Pt $\geqslant$ Co; the number of silver atoms (the most mobile element) migrating to the external surface corresponded to 25–50% of the total number of Ag atoms in the zeolite. From this these authors suggested that in the case of other zeolite forms, metals are mostly captured in the zeolite cavities. The values of L in Table 3 are greater than the free diameter of the zeolite cavities but it must be remembered that the values are averages and therefore do not preclude the existence of much smaller metallic clusters or crystallites in the zeolite cages. No lines due to Ru metal were observed in an X-ray diffraction pattern from sample A-2, probably due to a combination of the factors that the d spacings of the metal and the zeolite are very similar and that there is an insufficiency of well-formed crystals of adequate size present.

TABLE 4

Effect of Zeolite Structure on Metal Crystallite Size

Sample	L(% Ru)
A-2	1.79
X-1	0.16
X-2	0.26
Y-1	0.31
Y-4	0.36
L-2	1.28
L-4	1.06
M-4	0.64

The turnover numbers for hydrogenation of benzene at 353 K are listed in Table 5 and from Fig. 5 it is seen that with the exception of samples A-2 and L-2 the activity decreases regularly with increasing ruthenium content; a plot of the percentage of ruthenium as a function of the metal area A would again, with the exception of samples A-2 and L-2, show a similar smooth

dependence. Even though the activity of the catalysts can be rationalized by their crystallite sizes and dispersion factors it is interesting to note that samples A-2 and L-2 containing 9.1 and 4.3% ruthenium, respectively, are less active than samples X-1 and X-2 containing 24.2 and 13.9% ruthenium, respectively; if one expected an increase of dispersion with decrease of metal content in ruthenium zeolites then one would reasonably expect this order of catalytic activity to be reversed. In the case of A-2 if the hydrogenation were a diffusion process then zero activity would be expected since the A zeolite does not adsorb benzene; however, the fact that some activity is observed confirms that at least some of the ruthenium migrates to the exterior zeolitic surface on reduction. Penchev *et al.* (*32*) have reported dehydrogenation of cyclohexane on Ni, Na-A again showing the presence of metal aggregates on the external surface of this zeolite. Sample L-2 contains virtually the same amount of ruthenium by weight as sample Y-4 (the amounts are 4.3 and 4.4%, respectively) and consequently might be expected to show similar catalytic activity; also benzene and cyclohexane can diffuse

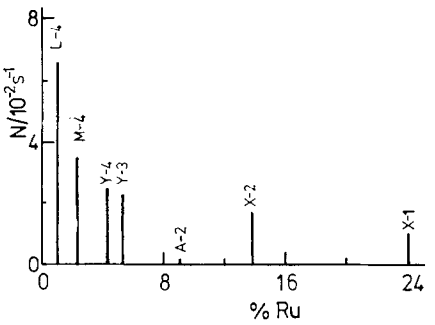

FIG. 5. Hydrogenation of benzene at 353 K; LHSV = 1; H/HC = 4.9.

through both the L and Y zeolites. At this point it should be remembered that the ruthenium in samples L-2 and A-2 was not as extensively hydrolyzed as in the other zeolites and the possibility arises that hydrolysis could play a role in the reduction and migration process; if this is the case then it would be more advantageous to prepare ruthenium zeolite reduction catalysts by using aqueous ruthenium trichloride solutions and thus ensuring hydrolysis than from solutions containing the hexa-aquo Ru(III) complex at low pH.

The fact that sample L-4 containing the least amount of ruthenium but also having

TABLE 5

Hydrogenation of Benzene at 353 K[a]

Catalyst	$N(10^{-2}\ s^{-1})$		
LHSV:	1	1	2
H/HC:	4.9	2.4	2.4
A-2	0.20 (0.13 × 10^{-3})	—	—
X-1	1.01 (0.67 × 10^{-3})	0.68	0.98
X-2	1.68 (1.11 × 10^{-3})	1.17	2.03
Y-1	2.34 (1.55 × 10^{-3})	—	2.77
Y-4	2.49 (1.65 × 10^{-3})	1.87	3.43
L-2	0.95 (0.63 × 10^{-3})	0.94	0.84
L-4	6.60 (4.37 × 10^{-3})	3.26	5.66
M-4	3.53 (2.34 × 10^{-3})	1.94	4.06

[a] Values in parentheses refer to turnover numbers defined as moles of benzene converted per hour per square meter of exposed ruthenium.

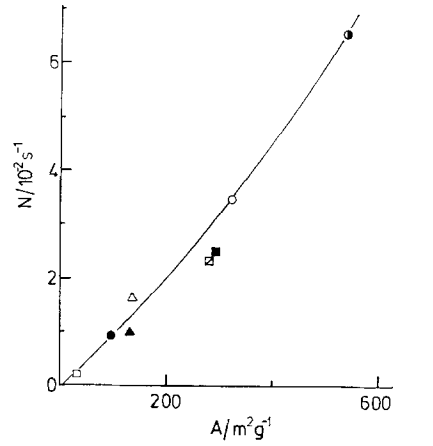

FIG. 6. Dependence of the catalytic activity of ruthenium A, X, Y, L and mordenite zeolites in the hydrogenation of benzene at 353 K on the surface area of the zeolitic ruthenium. (◑) L-4; (○) M-4; (■) Y-4; (▨) Y-1; (△) X-2; (▲) X-1; (●) L-2; (□) A-2; LHSV = 1; H/HC = 4.9.

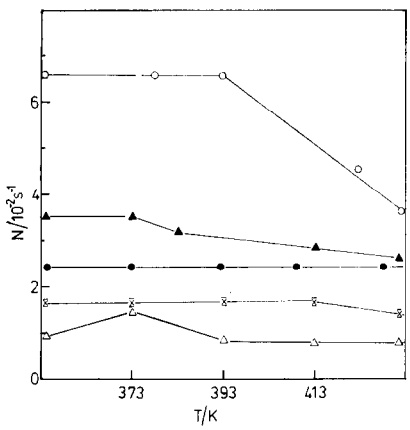

FIG. 7. Effect of temperature on hydrogenation of benzene; H/HC = 4.9. (○) L-4; (▲) M-4; (●) Y-4; (⧖) X-2; (△) L-2.

the smallest crystallite size is the most active of all the ruthenium zeolites studied emphasizes the dependence of the hydrogenation activity on metal dispersion. Figure 6 shows a clear correlation between the turnover number and the metal surface area for all the catalysts; this correlation assumes that the Ru metal accessible to hydrogen is also accessible to benzene and since a smooth curve is obtained for the several zeolites with widely differing pore structures and cation locations the assumption would seem to be justified; on the other hand an overestimation of the metal accessibility would lead to an underestimation of the turnover numbers. Consideration of Fig. 6 leads to the conclusion that the host zeolite lattice plays no part in the reduction of benzene by the ruthenium zeolites and that the activity is determined by the metal dispersion. In contrast with this several other workers have investigated the reduction of benzene using various metals and supports and have found varying effects due to crystallite size and the type of support. Gallezot *et al.* (*33*) have analyzed the activities for benzene hydrogenation and the poison sensitivity of platinum Y zeolites containing two different Pt dispersions: Pt agglomerates of 1 nm diameter fitting into the supercages and 1.5–2.0 nm crystallites occluded in the zeolite crystals. The formation of these latter crystallites involved a limited breakdown of the aluminosilicate framework and generated tricoordinated electron-deficient aluminum atoms. These unshielded aluminums in the immediate vicinity of the metal surface were postulated to be catalytically active in two ways, either through the provision of additional sites for benzene adsorption or by polarizing the benzene molecules and thus rendering them more reactive. On the other hand Aben *et al.* (*34*) who investigated the hydrogenation of benzene on Pt, Pd, and Ni as a function of metal particle size when supported on silica, alumina, silica–alumina and silica–magnesia concluded that the activity per exposed metal atom was independent of the metal crystallite size or of the support used. Coenen *et al.* (*35*) have reported the effect of crystallite size on activity per unit area in benzene hydrogenation for a range of silica supported nickel catalysts: from 5 nm down to 1.2 nm the specific activity increased with decreasing crystallite size as observed in the present investigation, but for still smaller crystallite size the activity appeared to go down, probably due to a support effect. Taylor and Staffin (*36*) in their investigation of the influence of support type and nickel level on the specific activity and other kinetic parameters for the hydrogenation of benzene used two different supports, silica and silica-alumina and the nickel concentration was varied in the 1–10% range; they observed a support effect at the lower nickel concentrations and the activity increased with increasing percentage of nickel.

Figure 7 shows the effect of varying temperature in the range 253–433 K on the hydrogenation; only samples X-2 and Y-4 maintain their activity steady throughout. There is a striking decrease in activity for the sample L-4 at temperatures above

393 K. Although much work has been done on the kinetics of benzene hydrogenation on various supported metals there is as yet no consensus of opinion on kinetic behavior and mechanism. Van Meerten *et al.* (*37*, *38*) have made a comprehensive analysis of a considerable amount of fragmented data available for nickel; they observed maxima in the reaction rate, which shifted depending on the conditions of hydrogen pressure and temperature, in the range 408–453 K but neither poisoning nor diffusion limitation nor approach to equilibrium could account for the maxima. In the present work, except for the A-2 and L-2 catalyst systems for which the percentage conversion was 3.4 and 14.5, respectively, all the other systems showed a conversion in excess of 99%; thus the fall in activity of the very active sample L-4 is possibly due to the attainment of equilibrium being much faster in this case.

CONCLUSION

Ruthenium exchanged A, X, Y, L, and mordenite zeolites are thermally stable molecular sieves. They are also stable to reduction at 723 K in flowing hydrogen and the metal crystallite size depends on the openness of the host zeolite lattice support and probably also on the degree of ruthenium hydrolysis. Benzene hydrogenation on the ruthenium zeolites seems to be a facile reaction with the activity being governed by the accessible metal surface area.

ACKNOWLEDGMENT

The second author thanks the National Science Council of Ireland for the award of a postdoctoral fellowship.

REFERENCES

1. Venuto, P. B., and Landis, P. S., *in* "Advances in Catalysis" (D. D. Eley, H. Pines and P. B. Weisz, Eds.), Vol. 18, p. 259. Academic Press, New York, 1968.
2. Turkevich, J., *Catal. Rev.* **1**, 1 (1968).
3. Venuto, P. B., *Advan. Chem. Ser.* **102**, 260 (1971).
4. Rabo, J. A., and Poutsma, M. L., *Advan. Chem. Ser.* **102**, 284 (1971).
5. Leach, H. F. *Ann. Rep. Progr. Chem.* **68A**, 195 (1971).
6. Kladnig, W. F. *Acta Cient. Venez.* **26**, 40 (1975).
7. Barrer, R. M., and Coughlan, B., "Molecular Sieves," pp. 233, 241. Butterworths, London, 1968 and references therein.
8. Coughlan, B., and Kilmartin, S., *J. Chem. Soc. Faraday I* **71**, 809 (1975).
9. Coughlan, B., and Shaw, R. G., *Proc. Roy. Ir. Acad.* **76B**, 191 (1976).
10. Coughlan, B., and McEntee, J. *Proc. Roy. Ir. Acad.* **76B**, 473 (1976).
11. Coughlan, B., and Larkin, P. M., *Chem. Ind.* 275 (1976).
12. Kikuchi, E., Tanaka, S., Yamazaki, Y., and Morita, Y., *Bull. Japan Petrol. Inst.* **16**, 95 (1974).
13. Allum, K. G., Hancock, R. D., Howell, I. V., Lester, T. E., McKenzie, S., Pitkethley, R. C., and Robinson, P. G., *J. Organomet. Chem.* **107**, 393 (1976).
14. Dalla Betta, R. A., Piken, A. G., and Shelef, M. *J. Catal.* **35**, 54 (1974).
15. Sinfelt, J. H., and Yates, D. J. C., *J. Catal.* **8**, 82 (1967).
16. Lam, Y. L., and Sinfelt, J. H., *J. Catal.* **42**, 319 (1976).
17. Forni, L., Ragaini, V., and Le Van, M., *J. Catal.* **33**, 153 (1974).
18. Amano, A., and Parravano, G., *in* "Advances in Catalysis" (D. D. Eley, W. G. Frankenburg, V. I. Komarewsky and P. B. Weisz, Eds.), Vol. 9, p. 716. Academic Press, New York, 1957.
19. Kubicka, H. *J. Catal.* **12**, 223 (1968).
20. Klimisch, R. L., and Taylor, K. C., *Ind. Eng. Chem. Product Res. Develop.* **14**, 26 (1975).
21. Coughlan, B., Carroll, W. M., and McCann, W. A., *Chem. Ind.* 527 (1976).
22. Coughlan, B., Carroll, W. M., and McCann, W. A., *J. Catal.* **45**, 332 (1976).
23. Hui, C. B., and James, B. R. *Canad. J. Chem.* **52**, 348 (1974).
24. Cotton, F. A., and Wilkinson, G., "Advanced Inorganic Chemistry" 3rd ed., p. 1007. Wiley (Interscience), New York, 1972.
25. Minachev, K. M., Antoshin, G. V., Shpiro, E. S., and Yusifov, Y. A., *Proc. Int. Congr. Catal. 6th*, pap. B2, (London) (1976).
26. Barrer, R. M., and Coughlan, B., "Molecular Sieves" p. 141. Butterworths, London, 1968.
27. Dyer, A., and Wilson, M. J., *Thermochim. Acta* **10**, 299 (1974).

28. Vucelic, V., Dondur, V., and Djurdjevic, P., *Thermochim. Acta* **14**, 341 (1976).
29. Weeks Jr., T. J., Hillery, H. F., and Bolton, A. P., *J. Chem. Soc. Faraday I* **71**, 2051 (1975).
30. Coughlan, B., and Carroll, W. M., *J. Chem. Soc. Faraday I* **72**, 2016 (1976).
31. Khvoschev, S. S., Zhdanov, S. P., and Shubaeva, M., *Izv. Akad. Nauk SSSR, Ser. Khim.* **5**, 1004 (1972).
32. Penchev, V., Minchev, H., Kanazirev, V., and Tsolovski, I., *Advan. Chem. Ser.* **102**, 434 (1971).
33. Gallezot, P., Datka, J., Massardier, J., Primet, M., and Imelik, B., *Proc. Int. Congr. Catal. 6th*, pap. A11, (London) (1976).
34. Aben, P. C., Platteeuw, J. C., and Stouthamer, B., *Proc. 4th Int. Congr. Catal., 4th*, pap. 31 (Moscow) (1968).
35. Coenen, J. W. E., Van Meerten, R. Z. C., and Rijnten, H. T., *Proc. Int. Congr. Catal., 5th*, pap. 45 (Florida) (1972).
36. Taylor, W. F., and Staffin, H. K. *Trans. Faraday Soc.* **63**, 2309 (1967).
37. Van Meerten, R. Z. C., and Coenen, J. W. E. *J. Catal.* **37**, 37 (1975).
38. Van Meerten, R. Z. C., Verhaak, A. C. M., and Coenen, J. W. E., *J. Catal.* **44**, 217 (1976).